



ISSN: 0067-2904

Determination of Timewise-Source Coefficient in Time-Fractional Reaction-Diffusion Equation from First Order Heat Moment

Qutaiba W.Ibraheem and M.S.Hussein*

Department of Mathematics, College of Science, University of Baghdad, Baghdad, Iraq

Received: 18/2/2023

Accepted: 1/4/2023

Published: 30/3/2024

Abstract

This article aims to determine the time-dependent heat coefficient together with the temperature solution for a type of semi-linear time-fractional inverse source problem by applying a method based on the finite difference scheme and Tikhonov regularization. An unconditionally stable implicit finite difference scheme is used as a direct (forward) solver. While by the MATLAB routine *lsqnonlin* from the optimization toolbox, the inverse problem is reformulated as nonlinear least square minimization and solved efficiently. Since the problem is generally incorrect or ill-posed that means any error inclusion in the input data will produce a large error in the output data. Therefore, the Tikhonov regularization technique is applied to obtain stable and accurate results. Finally, to demonstrate the accuracy and effectiveness of our scheme, two benchmark test problems have been considered, and its good working with different noise levels.

Keywords: Implicit finite difference scheme (IFDS), Tikhonov technique, Caputo fractional derivative, Time-fractional source inverse problem, Stability analysis.

تحديد معامل المصدر الزمني في معادلة التفاعل والانتشار الزمني من عزم الحرارة من الدرجة الأولى

قتيبة وادي ابراهيم, محمد صباح حسين*

قسم الرياضيات، كلية العلوم، جامعة بغداد، بغداد، العراق.

الخلاصة

تهدف هذه المقالة إلى تحديد معامل الحرارة المعتمد على الوقت جنباً إلى جنب مع حل درجة الحرارة لنوع من مشكلة المصدر العكسي الجزئي شبه الخطي من خلال تطبيق طريقة تعتمد على مخطط الفروق المحدودة وتنظيم Tikhonov. تم استخدام مخطط الفرق المحدود الضمني المستقر غير المشروط كحل مباشر (أمامي). بينما تمت إعادة صياغة المسألة العكسية على أنها تصغير غير خطي للمربع الصغرى وحلها بكفاءة بواسطة MATLAB الروتين *lsqnonlin* من صندوق أدوات الأمثلية. نظراً لأن المشكلة بشكل عام معتلة أو غير صحيحة، أي أن إدراج أي خطأ في بيانات الإدخال سيؤدي إلى حدوث خطأ كبير في بيانات الإخراج، لذلك تم تطبيق تقنية تنظيم Tikhonov للحصول على نتائج مستقرة ودقيقة. أخيراً، لإثبات دقة وفعالية مخططنا، تم النظر في مثالين لاختبار مجموعة العلامات، وكان عملها جيد مع مستويات ضوضاء مختلفة.

1. Introduction

The use of fractional partial differential equations to model many systems and processes is still ongoing and their applications are very wide [1, 2]. They have many types, the most

*Email: gateeba.wadi1103a@sc.uobaghdad.edu.iq

important is the diffusion equation of fractional order that was used for the first time in physics [3] to describe the diffusion in media using fractal geometry. However, sometimes, a part of the data may not be given. These data are source terms, diffusion coefficients, initial data, boundary data, and e.t. Therefore, these data must be determined by additional information, and this is called fractional inverse problems. Work and study of direct problems of PDE have become widespread. In another hand, work on inverse problems is very little and more recent, articles on this aspect are few and very limited, see [4 – 11]for some examples of work to solve inverse problems.

In this article, we consider the time-fractional inverse source problem to reconstruct the unknown time-source coefficient $c(t)$ in the following time-fractional reaction–diffusion equation:

$$D_t^\alpha u(x, t) = u_{xx} - a(t)u(x, t) + c(t)F(x, t, u), \quad (x, t) \in (0,1) \times (0, T]. \quad (1)$$

The initial condition

$$u(x, 0) = \varphi(x), \quad x \in [0,1], \quad (2)$$

and nonlocal boundary conditions;

$$u(0, t) = u(1, t); \quad u_x(1, t) = 0, \quad t \in [0, T], \quad (3)$$

and integral over determination condition

$$\int_0^1 xu(x, t)dx = e(t), \quad 0 \leq t \leq T, \quad (4)$$

where $F(x, t, u)$, $\varphi(x)$ and $e(t)$ are given functions, $a(t)$ is given positive function, $c(t)$ is unknown time-dependent coefficient. Mathematically, Eq. (1) is a parabolic fractional partial differential equation where $u(x, t)$ represents the concentration of one substance, u_{xx} is a diffusion term, $a(t)u(x, t) + c(t)F(x, t, u)$ represents the reaction term where $F(x, t, u)$ is a non-linear source term and $a(t) > 0$ can be regarded as a control parameter. $D_t^\alpha u(x, t)$ is the Caputo time-fractional derivative of order $0 < \alpha < 1$, [12]:

$$D_t^\alpha u = \frac{1}{\Gamma(1-\alpha)} \int_0^t (t-s)^{-\alpha} \frac{\partial u(x,s)}{\partial s} ds, \quad 0 \leq t \leq T,$$

The unique solvability for the inverse problem (1)-(4) is established in [12] and reads under the following assumptions:

(A1) $a \in C[0, T]$ is a positive function and $M_a = \|a\|_{C(0,T)}$.

(A2) $\phi \in C^4[0, 1]$ such that $\phi(0) = \phi(1), \phi'(1) = 0, \phi''(0) = \phi''(1), \phi'''(1) = 0$.

(A3) Let the function $F(x, t, u)$ be continuous with respect to all arguments in $(0,1) \times (0, T] \times R$ and satisfies the following conditions:

1. $F(\cdot, t, u) \in C^4[0, 1], t \in [0, T], F(x, t, u)|_{x=0} = F(x, t, u)|_{x=1}$,
2. $F_x(x, t)|_{x=1} = 0, F_{xx}(x, t)|_{x=0} = F_{xx}(x, t)|_{x=1}, F_{xxx}(x, t)|_{x=1} = 0$.
3. There exists a nonnegative function $b(x, t)$ such that for each $u, \tilde{u} \in R$ and $(x, t) \in (0,1) \times (0, T]$,

$$\left| \frac{\partial^r}{\partial x^r} F(x, t, u) - \frac{\partial^r}{\partial x^r} F(x, t, \tilde{u}) \right| \leq b(x, t)|u - \tilde{u}|, \quad r = 0, 1, 2$$

where $b \in L^2((0,1) \times (0, T]), \max_{0 \leq t \leq T} \|b(\cdot, t)\|_{L^2(0,1)} < \infty$;

4. $M_F = \max\left\{ \left\| \frac{\partial^r}{\partial x^r} F(\cdot, \cdot, u) \right\|_{L^2((0,1) \times (0,T])}; r = 0, 1, 2 \right\}$.

5. There exists a positive constant F_m such that $|\int_0^1 xF(x, t, u) dx| > F_m$ for each $t \in [0, T]$ and uniformly to $u \in R$.

(A4) $E \in C([0, T])$ and $E(0) = \int_0^1 x\phi(x) dx$.

In recent years, inverse source problems have received great attention from researchers, as they have been studied in many articles. Wei and Zhang [13] solved the time-fractional time-dependent source problem by a method based on the separation of variables and Duhamel's principle and Tikhonov regularization. Y. Zhang and X. Xu [14] used the eigen function method and Tikhonov regularization to solve the fractional inverse source problem (FISP) for the one-dimensional time-fractional diffusion equation. Wang, Yamamoto and Han [15] identified a space-dependent coefficient-source from data at the final time by using a reproducing kernel space method. By using a modified quasi-boundary value method, Wei and Wang [16] determined the space-dependent source parameter by using the final data. Tatar and Ulusoy [17] determined an inverse space-dependent coefficient-source for nonlocal ISP for a one-dimensional time-fractional diffusion equation. Tuan, Long and Thinh [18] solved an ISP for a time-fractional diffusion equation and determined an unknown source by using the Tikhonov regularization method (TRM). Tuan and Nane [19] solved an ISP for a fractional diffusion equation for the random case and determined a source parameter. Jian, Li, Liu and Yamamoto [20] proposed an iterative threshold algorithm and found the numerical solution to the inverse source problem, they reformulated it as an optimization problem. Ma, Prakash and Deiveegan [21] identified the unknown space-dependent source term in an ISP for time-fractional diffusion equation with variable coefficients in a bounded domain by generalized Tikhonov regularization method (GTRM). By using the fractional Tikhonov regularization method (FTRM), Xiong and Xue [22] solved ISP for the time-fractional diffusion equation and identified a space-dependent source. Djennadi, Smina, Inc, Osman, Gómez and Abu Arqub [23] solved the ISP of the Atangana-Baleanu-Caputo fractional diffusion equation by using the Tikhonov regularization method (TRM). The later authors also [24] solved the inverse source problem of the time-space fractional diffusion equation by using a numerical scheme in the RKHS approach and determining of state variable and source parameter. By using TRM, Liu, Songshu, Sun, and Feng [25] solved ISP for a fractional diffusion equation with a fractional Riemann-Liouville derivative. By using the generalized quasi-boundary value method, Wei, Ting, and Luo [26] solved ISP for a time-fractional wave equation and identified a space-dependent source by using the final time data. Molaei, Tahereh, and Shahrezaei [27] solved ISP for time-fractional differential equations by the DMLPG method. Ebru, et.al [28] solved a time-fractional inverse problem for a parabolic equation by a finite difference scheme.

In our article, a stable numerical solution to problem (1) - (4) should be obtained by using implicit finite difference (IFD) with Tikhonov regularization [29]. First, we apply (IFD) to obtain the direct solution to problem (1)-(3). Next, we use the Tikhonov regularization to stabilize this problem.

The article consists of six sections: (IFDS) is given in section 2 to obtain the numerical solution of problems (1)-(3). Section 3 is developed to investigate the stability and convergence of the numerical procedure. The numerical approach to solving (TFSIP) of equations (1)-(4) is given in section 4. In section 5, some experiments are provided. The end section gives the conclusions for this work.

2. Fractional Finite Differences Scheme (FFDS)

In this section, we give a direct solution method to problem (1)-(3). We start by letting M and N are two positive integers. Consider a regular grid in $I = [0,1] \times [0, T]$ as:

$$\Omega = \{(x_i = ih, t_j = jk), j = 0, 1, 2, \dots, N; i = 0, 1, 2, \dots, M\},$$

The step length in space and time are $h = 1/M$ and $k = T/N$, respectively. In addition, suppose

$$u_i^j := u(x_i, t_j), \quad a_j := a(t_j), \quad c_j := c(t_j), \quad F_i^j := F(x_i, t_j, u(x_i, t_j)),$$

$$\varphi_i := \varphi(x_i), \quad E_j := E(t_j) \quad \text{for } j = 0, 1, 2, \dots, N; \quad i = 0, 1, 2, \dots, M,$$

$$u_{xx}(x_i, t_j) \approx \frac{u_{i-1}^j - 2u_i^j + u_{i+1}^j}{h^2} \quad \text{for } j = 0, 1, 2, \dots, N; \quad i = 1, 2, \dots, M$$

and

$$u_x(x_i, t_j) \approx \frac{u_{i-1}^j - u_{i+1}^j}{2h}$$

The discrete form of the term $D_t^\alpha u$ that is introduced in [4] is defined as the following:

$$D_t^\alpha u(x_i, t_j) \approx q_{\alpha,k} \sum_{k=1}^j w_j^\alpha (u_i^{j-k+1} - u_i^{j-k}) \tag{5}$$

where $q_{\alpha,k} = \frac{k^{-\alpha}}{(1-\alpha)\Gamma(1-\alpha)}$.

We must note that w_j^α satisfies the following fact:

$$w_j^\alpha = (j)^{1-\alpha} - (j-1)^{1-\alpha}, \quad j = 1, 2, \dots, N.$$

From equation's (2) and (3), we obtain the following discrete form of boundary

$$u_0^j = u_M^j, \quad u_{M+1}^j = u_{M-1}^j, \quad j = 0, 1, 2, \dots, N, \tag{6}$$

and the discrete initial condition; so as;

$$u_i^0 = \varphi_i, \quad i = 0, 1, 2, \dots, M. \tag{7}$$

By using equations (5), (6) and (7), we get the following formula for governing equation (1) :

$$q_{\alpha,k} \sum_{k=1}^j w_j^\alpha (u_i^{j-k+1} - u_i^{j-k}) = \gamma [u_{i-1}^j - 2u_i^j + u_{i+1}^j] - a_j u_i^j + c_j F_i^j$$

where $\gamma = \frac{1}{h^2}$, $i = 1, 2, \dots, M-1$.

$$q_{\alpha,k} \sum_{k=1}^j w_j^\alpha (u_i^{j-k+1} - u_i^{j-k}) = [\gamma u_{i-1}^j - (2\gamma + a_j)u_i^j + \gamma u_{i+1}^j] + c_j F_i^j.$$

Or

$$q_{\alpha,k} w_1^\alpha (u_i^1 - u_i^0) + q_{\alpha,k} \sum_{k=2}^j w_k^\alpha (u_i^{j-k+1} - u_i^{j-k}) = [\gamma u_{i-1}^j - (2\gamma + a_j)u_i^j + \gamma u_{i+1}^j] + c_j F_i^j \tag{8}$$

We must note that w_j^α satisfies the following fact:

$$1 = w_1^\alpha > w_2^\alpha > w_3^\alpha > \dots \rightarrow 0, \quad j = 1, 2, \dots, N.$$

We apply equation (8) when $i = 1, 2, \dots, M-1, M$, we have:

- At the first-time level ($j = 1$),

$$-\gamma u_{i-1}^1 + (2\gamma + a_1 + q_{\alpha,k} w_1^\alpha) u_i^1 - \gamma u_{i+1}^1 = c_1 F_i^1 + q_{\alpha,k} w_1^\alpha \varphi_i, \tag{9}$$

and from (8) and (6) at $i = M$, we have:

$$-2\gamma u_{M-1}^1 + (2\gamma + a_1 + q_{\alpha,k} w_1^\alpha) u_M^1 = c_1 F_M^1 + q_{\alpha,k} w_1^\alpha \varphi_M \tag{9a}$$

- At ($j = 2, 3, \dots, N$),

$$-\gamma u_{i-1}^j + (2\gamma + a_j + q_{\alpha,k} w_1^{(\alpha)}) u_i^j - \gamma u_{i+1}^j = c_j F_i^j + q_{\alpha,k} \sum_{k=1}^{j-1} (w_k^\alpha - w_{k+1}^\alpha) u_i^{j-k} + q_{\alpha,k} w_j^\alpha \varphi_i \tag{10}$$

and from (8) and (6) at $i = M$, we have:

$$-2\gamma u_{M-1}^j + (2\gamma + a_j + q_{\alpha,k} w_1^{(\alpha)}) u_M^j = c_j F_M^j + q_{\alpha,k} \sum_{k=1}^{j-1} (w_k^\alpha - w_{k+1}^\alpha) u_i^{j-k} + q_{\alpha,k} w_j^\alpha \varphi_M \tag{10a}$$

Using equations (9), (9a), (10) and (10a), for $j = 1, \dots, N$ and $i = 1, 2, \dots, M$, it can be written in more compact form:

$$AU^1 = c_1 F^1 + q_{\alpha,k} U^0,$$

$$AU^j = c_j F^j + q_{\alpha,k} D_i^{j-1}, j = 2, \dots, N$$

where

$$A = \begin{bmatrix} (2\gamma + a_j + q_{\alpha,k} w_1^\alpha) & -\gamma & 0 & 0 & \dots & 0 & 0 & 0 \\ -\gamma & (2\gamma + a_j + q_{\alpha,k} w_1^\alpha) & -\gamma & 0 & \dots & 0 & 0 & 0 \\ 0 & -\gamma & (2\gamma + a_j + q_{\alpha,k} w_1^\alpha) & -\gamma & \dots & 0 & 0 & 0 \\ \vdots & \vdots & \vdots & \vdots & \vdots & \vdots & \dots & \vdots \\ 0 & 0 & 0 & -\gamma & (2\gamma + a_j + q_{\alpha,k} w_1^\alpha) & -\gamma & 0 & \\ 0 & 0 & 0 & \dots & 0 & -\gamma & (2\gamma + a_j + q_{\alpha,k} w_1^\alpha) & -\gamma \\ 0 & 0 & 0 & \dots & 0 & 0 & 0 & -2\gamma & (2\gamma + a_j + q_{\alpha,k} w_1^\alpha) \end{bmatrix}$$

$$F^j = [F_1^j, F_2^j, \dots, F_N^j]^t, j = 1, 2, \dots, N,$$

where u_i^0 is computed from equation (7). Also, we have $U^j = [u_1^j, u_2^j, \dots, u_M^j]^t$,

$$D_i^{j-1} = \sum_{k=2}^{j-1} (w_k^\alpha - w_{k+1}^\alpha) u_i^{j-k} + w_j^\alpha u_i^0.$$

Finally, discretize integral condition (4) by using the trapezoidal rule as:

$$e(t_j) = \frac{1}{2M} \left(x_0 u_0^j + x_M u_M^j + 2 \sum_{k=1}^{M-1} x_k u_k^j \right), j = 0, 1, 2, \dots, N.$$

3. Stability and Convergence

Here, we use the Von Neumann method [30] to prove the stability of the scheme (8). Let the solution of the equations (9) and (10) with $\varphi(x)$ be U and \tilde{U} is the solution to the perturbed data $\tilde{\varphi}(x)$.

Define the error $E = \tilde{U} - U, E^j = \tilde{U}^j - U^j = (e_0^j, e_1^j, \dots, e_M^j)^T$ i.e. $e_i^j = \tilde{u}_i^j - u_i^j, j = 0, 1, 2, \dots, N, i = 0, 1, 2, \dots, M$.

Theorem 1. The FDM scheme (8) is unconditionally stable.

Proof:

Assume $e_i^j = \xi_j e^{i\beta h}$, where β is a real spatial number [31] and $\tilde{t} = \sqrt{-1}$. From equation (9), we have

$$-\gamma \xi_1 e^{i\beta(i-1)h} + (2\gamma + \tilde{a}_1 + q_{\alpha,k} w_1^\alpha) \xi_1 e^{i\beta i h} - \gamma \xi_1 e^{i\beta(i+1)h} = \xi_0 e^{i\beta i h},$$

where $\tilde{a} = \max_{t \in [0, T]} |a(t)|$, which can be reduced to

$$-\gamma \xi_1 e^{-i\beta h} + (2\gamma + \tilde{a}_1 + q_{\alpha,k} w_1^\alpha) \xi_1 - \gamma \xi_1 e^{i\beta h} = \xi_0,$$

Or,

$$\xi_1 = \frac{\xi_0}{-\gamma e^{-i\beta h} + (2\gamma + \tilde{a}_1 + q_{\alpha,k} w_1^\alpha) - \gamma e^{i\beta h}}$$

which implies

$$\xi_1 = \left(\frac{1}{2\gamma(1 - \cos \beta h) + \tilde{a}_1 + q_{\alpha,k} w_1^\alpha} \right) \xi_0. \tag{11}$$

Since $2\gamma(1 - \cos \beta h) + \tilde{a}_1 + q_{\alpha,k} w_1^\alpha \geq 1$, it follows that $\xi_1 \leq \xi_0$.

Now, from equation (10) when $j \geq 2$ and substituting $e_i^j = \xi_j e^{i\beta i h}$, we have

$$-\gamma \xi_j e^{-i\beta h} + (2\gamma + a_j + q_{\alpha,k} w_1^\alpha) \xi_j - \xi_j e^{i\beta h} = q_{\alpha,k} \sum_{k=1}^{j-1} (w_k^\alpha - w_{k+1}^\alpha) \xi_{j-k} + q_{\alpha,k} w_j^\alpha \xi_0$$

$$(-\gamma e^{-i\beta h} + (2\gamma + a_j + \sigma_{\alpha,k} w_1^\alpha) - \gamma e^{i\beta h}) \xi_j = q_{\alpha,k} \sum_{k=1}^{j-1} (w_k^\alpha - w_{k+1}^\alpha) \xi_{j-k} + q_{\alpha,k} w_j^\alpha \xi_0$$

$$\xi_j = \frac{q_{\alpha,k} \sum_{k=1}^{j-1} (w_k^\alpha - w_{k+1}^\alpha) \xi_{j-k} + q_{\alpha,k} w_j^\alpha \xi_0}{(2\gamma(1 - \cos \beta h) + \tilde{a}_j + q_{\alpha,k} w_1^\alpha)}$$

By induction, we have $\xi_N \leq \xi_{N-1} \leq \dots \leq \xi_1 \leq \xi_0$. Thus $|e_i^j| \leq |e_i^{j-1}|$, for all j . This completes the proof of the unconditional stability of the scheme (8).

Now, we must prove the convergent. Consider $\|E^j\|_2^2 = h \sum_i |e_i^j|^2$. This Euclidean norm of the perturbation [31]. Therefore, the stability condition can be written as:

$$\|E^j\|_2 \leq \|E^{j-1}\|_2, j = 1, 2, \dots, N \tag{15}$$

This relation implies that $\|E^j\|_2 \leq \|E^0\|_2$, Equation (8) can be rewritten as:

$$AU^j = \mathcal{M}U^{j-1},$$

where \mathcal{M} is the difference operator defined as:

$$(\mathcal{M}U^{j-1})_i = \sum_{k=1}^{j-1} (w_k^\alpha - w_{k+1}^\alpha)(U^{j-k})_i + w_j^\alpha (U^0)_i$$

From $AE^j = \mathcal{M}E^{j-1}$, we have $E^j = A^{-1}\mathcal{M}E^{j-1}$, by considering equation (15), gives

$$\|A^{-1}\mathcal{M}E^{j-1}\|_2 \leq \|E^{j-1}\|_2. \tag{16}$$

That is the operator $A^{-1}\mathcal{M}$ is a non-expansive.

Now, take $A - \mathcal{M} = R$, where R is the difference equation at mesh point (i, k) th. So if R tends to zero ($R \rightarrow 0$), the scheme (8) is consistent [33,34].

Now, define $e^j = u^j - U^j$, where U is the numerical solution and u is the exact solution, then we have [32].

$$A e^j = \mathcal{M}e^{j-1} + R^j \tag{17}$$

Therefore, from equation (17), we can write

$$\|e^j\|_2 \leq \|A^{-1}\mathcal{M}e^{j-1}\|_2 + \|A^{-1}\|_2 \|R^j\|_2 \tag{18}$$

Because $A^{-1}\mathcal{M}$ is non-expansive, then from equation (18) we have

$$\|e^j\|_2 \leq \|e^{j-1}\|_2 + \|A^{-1}\|_2 \|R^j\|_2 \tag{19}$$

Thus, by induction, we have

$$\|e^j\|_2 \leq \|A^{-1}\|_2 \sum_{k=1}^j \|R^k\|_2 \tag{20}$$

This inequality shows that if $\|A^{-1}\|_2$ for equations (9) – (10) is bounded, then, the error $\|e^j\|_2 \rightarrow 0$. This completes the proof of the convergence of the proposed method.

3.1 Numerical Example for Direct Problem

Here, an example is given for the direct problem, that is when the coefficient $c(t)$ is known, to validate, stability, and accuracy for (FFDS).

Example 1 Consider solving the problem (1)-(3) with the data:

$$a(t) = 100e^{100t}, t \in [0,1],$$

$$c(t) = e^t, t \in [0,1],$$

$$\varphi(x) = 0, x \in [0,1],$$

$$F(x, t, u) = \frac{1}{\Gamma(2-\alpha)} t^{-\alpha} u - (2-12x^2)t + 100e^{100t}u, (x, t) \in [0,1] \times [0,1],$$

where $u(x, t) = x^2(1 - x^2)t$ is the exact solution. Figure 1 shows the absolute error between the exact and numerical solutions of $u(x, t)$ when $\alpha \in \{0.25, 0.5, 0.75\}$, $M = N = 40$. And, one can see from this 3D figure excellent agreement is obtained. Figure 2 shows the exact and numerical solutions for the thermal energy $e(t)$

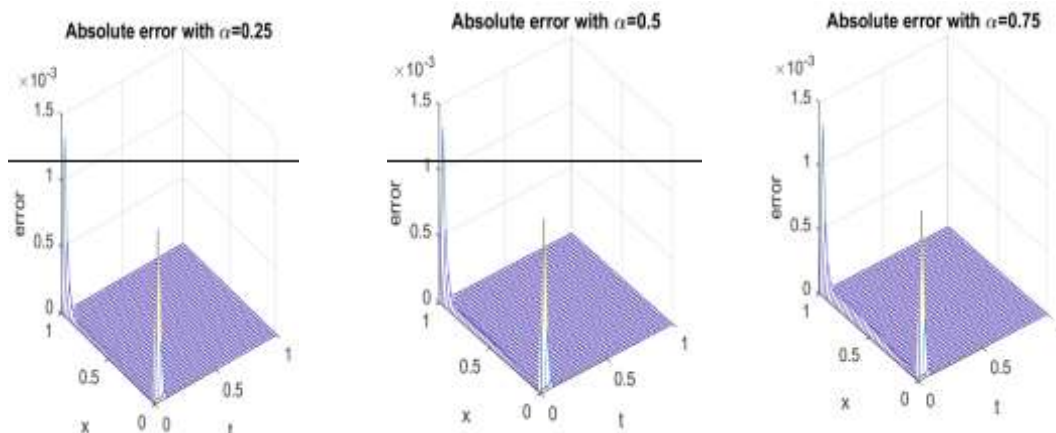


Figure 1: The absolute error between the true and numerical solutions of $u(x, t)$ when $\alpha \in \{0.25, 0.5, 0.75\}$ for Example 1.

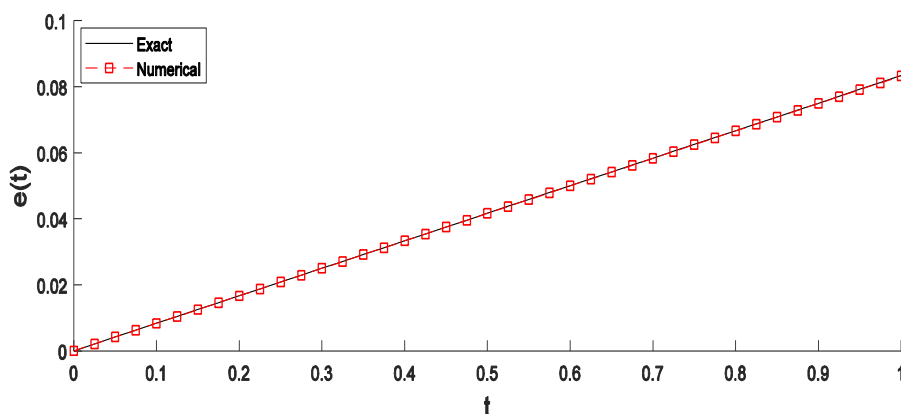


Figure 2: The required output $e(t)$, with $N = M = 40$, for Example 1 with $\alpha = 0.5$.

4. Numerical Procedure for Time-Fractional Source Inverse Problem (TFSIP)

We aim to find the numerical solution for problem (1)-(4) which is described in Section 2. We want to find stable reconstructions for the unknown coefficient $c(t)$ of the one-dimensional semi-linear time-fractional equation together with $u(x, t)$ to fulfill equations (1)-(4).

Observe that from (1) and (4), we have:

$$c(t) = \frac{D_t^\alpha e(t) + a(t)e(t)}{\int_0^1 xF(x,t,u)dx}$$

Therefore, by using $t = 0$ in the above equation,

$$c(0) = \frac{D_t^\alpha e(0) + a(0)e(0)}{\int_0^1 xF(x, 0, \varphi(x))dx},$$

which is a constant initial guess. Now, we recast this problem as a nonlinear minimization problem. In the other words, we minimize the gap between measured data and computed solutions. The Tikhonov regularization functional can be found by imposing the condition (4):

$$F(c) = \left\| \int_0^1 xu(x, t)dx - e(t) \right\|^2 + \beta \|c(t)\|^2, \tag{21}$$

or in discretized form,

$$F(\underline{c}) = \sum_{j=1}^N \left(\int_0^1 x u(x, t_j) dx - e(t_j) \right)^2 + \beta \sum_{j=1}^N c_j^2, \quad (22)$$

where $\beta > 0$ represents a parameter of regularization. The *lsqnonlin* routine is used to achieve a minimum objective F function, for more details see [35]. *Lsqnonlin*'s routine starts from $c(0)$ and tries to find a minimum of the scalar function of several variables, given the constraints, for more details see [4]. We take the parameters of the routine as:

- *Maximum number of iterations* = $10^2 \times (\text{number of variables})$.
- *Solution and Objective function tolerances* = 10^{-15} .

The fractional inverse problem (1)-(4) is tested subject to both noisy measurement and exact data (4). The noise-contaminated is simulated as:

$$e^\epsilon(t_j) = e(t_j) + \epsilon_j, \quad j = \overline{0, N} \quad (23)$$

where ϵ represents the Gaussian random vector with a mean equal to zero and standard deviation is given by:

$$\sigma = p \times \max_{t \in [0, T]} |e(t)|, \quad (24)$$

where p represents the percentage of noise. We anticipate the *normrnd* built in function to generate the random variables $\underline{\epsilon} = (\epsilon_j), j = \overline{0, N}$ as :

$$\underline{\epsilon} = \text{normrnd}(0, \sigma, N). \quad (25)$$

5. Results and Discussions

The Root Means Square Error (RMSE) has been used to check the accuracy of numerical results after employing the Tikhonov regularization technique, and its formula is given as follows:

$$RMSE(c) = \sqrt{\frac{1}{N} \sum_{j=1}^N (c_{\text{numerical}}(t_j) - c_{\text{exact}}(t_j))^2}, \quad (26)$$

For simplicity, we fix $T = 1$ in all following numerical experiments.

Example 5.1: (Smooth Coefficient) Consider the fractional inverse problem (1)-(4) with input data in Example 1 of the direct problem with the $e(t) = \frac{1}{12}t, t \in [0, 1]$ and the coefficient $c(t)$ is unknown. The initial guess is taken as $c_0 = 1$. Figure 3 shows the numerical solution of the time-dependent source function from first order heat moment (4) in comparison with the exact solution ($c(t) = e^t$) obtained by solving the inverse problem with the input data in Example 1 using the FFDS, which is described in Section 2, with $M = N \in \{10, 20, 40\}$. In Figure 4, the counter of iterations required to reach the convergence of the functional (22) to a very low threshold value of $O(10^{-15})$ is plotted with $M = N \in \{10, 20, 40\}$. From this figure, it can be observed a speed convergence was achieved in 5 iterations only to reach a very low value of order $O(10^{-15})$. However, the problem remains ill-posed and has to be regularized.

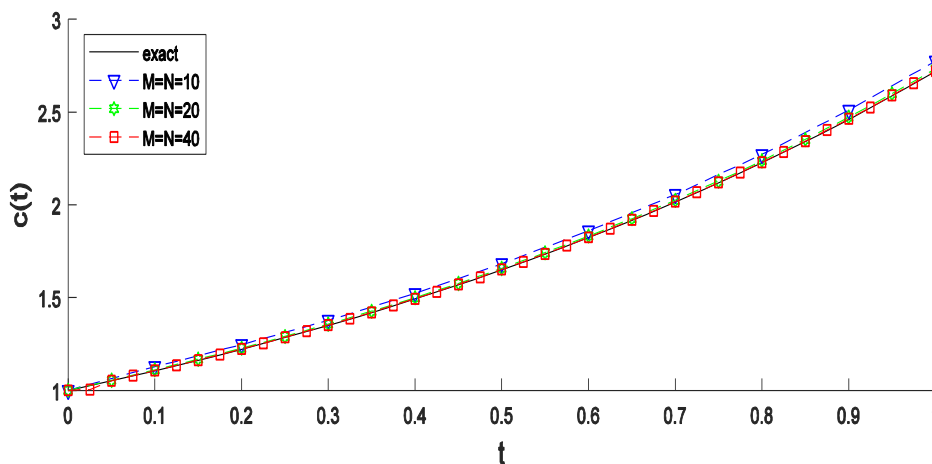


Figure 3: The numerical solutions for time-dependent source $c(t)$ and exact value ($c(t) = e^t$) for Example 5.1 with $p = 0$ and $\beta = 0$.

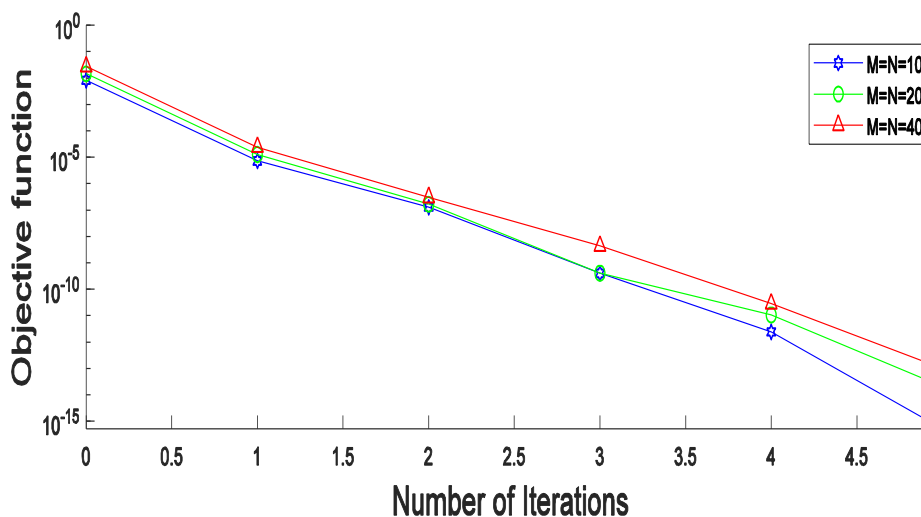


Figure 4: Objective function (22) for Example 5.1 when $\beta = 0$ and with = 0% .

Next, we fix $N = M = 40$ and start our investigation with cases (i) no noise ($p = 0\%$) and (ii) noise ($p = 10\%$), included in the measurement data (4). Figure 5 explains the comparisons of numerical results with the exact solution for $c(t)$ with no regularization ($\beta = 0$) and (a) no noise ($p = 0\%$) and (b) with noise $p \in \{3,10\}\%$. Subfigure (a) investigates the convergence of the numerical solution for $c(t)$, while we note the results in subfigure (b) are unstable and inaccurate and this is expected.

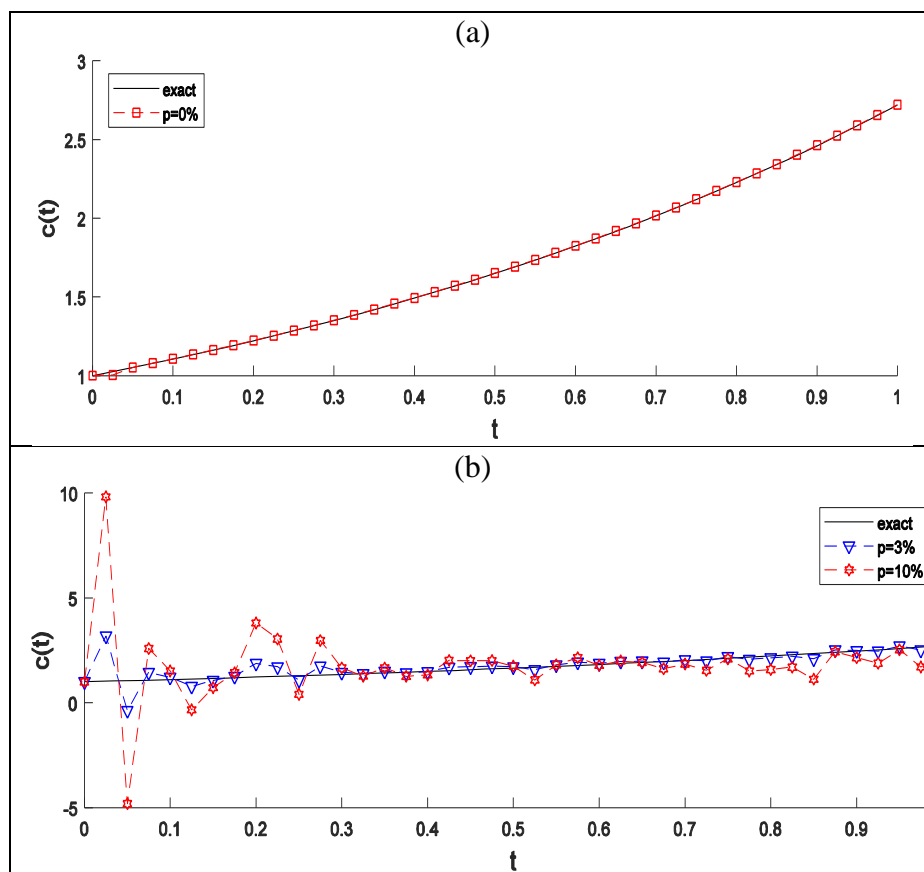


Figure 5: Reconstructed $c(t)$ for Example 5.1 with $\beta = 0$ and (a) $p = 0\%$ and (b) $p \in \{3,10\}\%$ noise.

The reconstructed $c(t)$ are presented in Figure 6 after applying the Tikhonov regularization with $p = 10\%$ and $\beta \in \{10^{-4}, 10^{-5}, 10^{-6}\}$. The speed converges minimization of the objective function (22), as a function of the number of iterations, for $\beta \in \{10^{-i}, i = 4,5,6\}$ shown in Figure 7. The 3D graph of absolute error between true solution and numerical solution for temperatures $u(x, t)$ is plotted in Figure 8 with (a) $p = 3\%$ and (b) $p = 10\%$ with (i, iv) $\beta = 10^{-4}$, (ii, v) $\beta = 10^{-5}$ and (iii, vi) $\beta = 10^{-6}$. Next, in Table1, we compute the *RMSE* errors (25) for $\beta \in \{0, 10^i, i = 3,4,5,6\}$ and $p \in \{3, 5, 10\}\%$. Clearly, from Figures 5,6,8 and Table 1, it can be seen that there is good agreement and convergence between the numerical solutions of $c(t)$ and $u(x, t)$ with their corresponding exact solutions, where p decreases from 10 % to 3% and then to 0%.

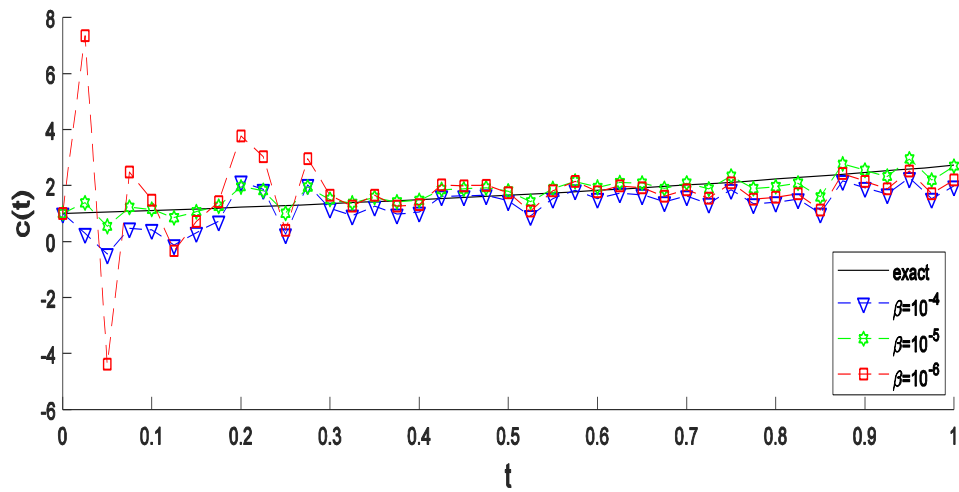


Figure 6: The reconstructed $c(t)$ for Example 5.1. with $p = 10\%$ and different amounts for β .

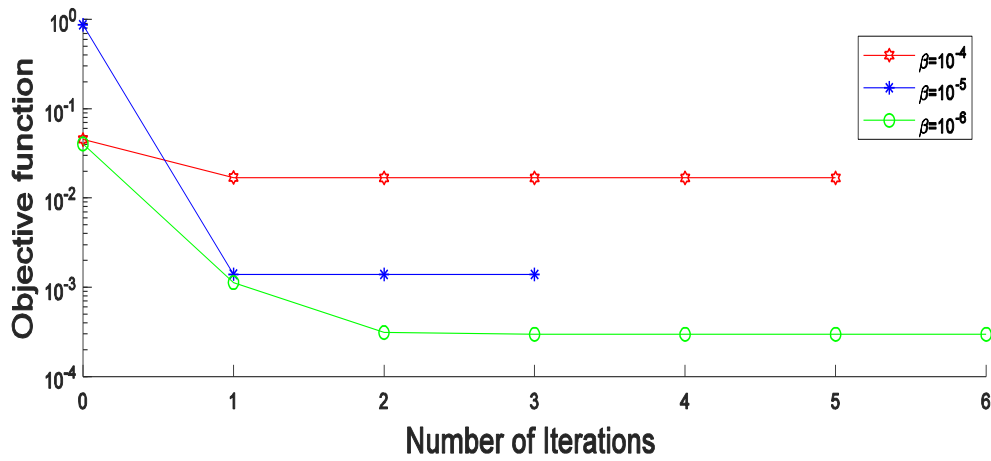
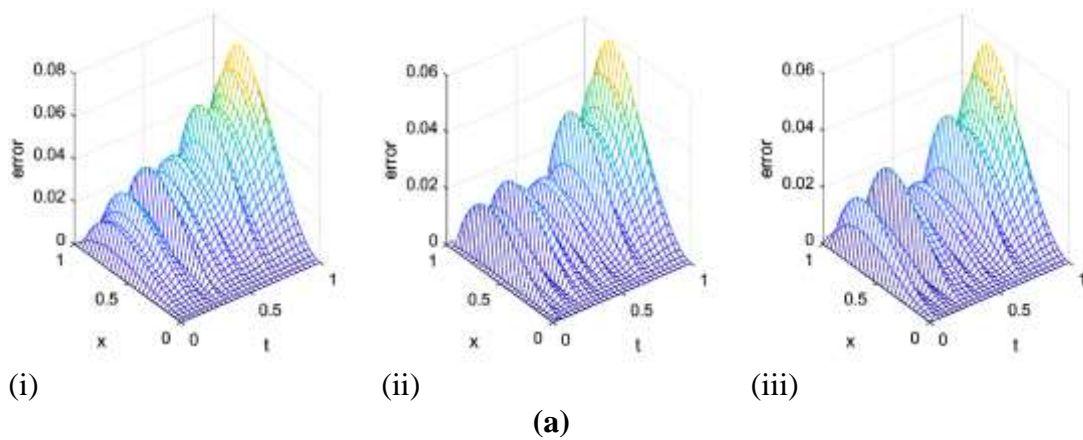


Figure 7: Objective function (22), with different values for β and $p = 10\%$, for Example 5.1



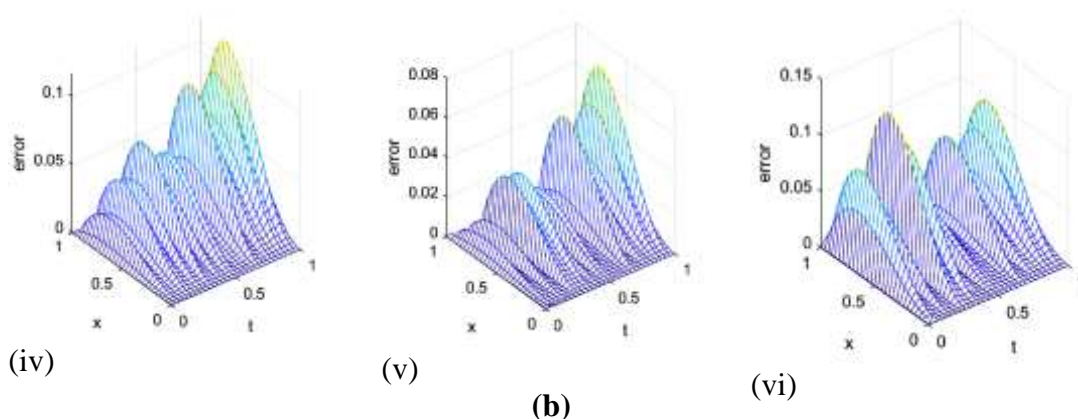


Figure 8: The absolute error between the exact and numerical solutions of $u(x, t)$ for Example 5.1 with different values of p and β

Table 1: The $RMSE$ value (25) for various amounts of noise $p \in \{3,5,10\}\%$ and various regularization parameters $\beta \in \{0, 10^{-i}, i = 3,4,5,6\}$ for Example 5.1.

$RMSE(c)$			
	$p = 3\%$	$p = 5\%$	$p = 10\%$
$\beta = 0$	0.4513	0.6272	1.8438
$\beta = 10^{-4}$	0.3869	0.5416	0.6748
$\beta = 10^{-5}$	0.2655	0.4589	0.3111
$\beta = 10^{-6}$	0.3819	0.6368	1.5274

Example 5.2: (Non-Smooth Coefficient)

In this example, the time-fractional inverse source problem that is represented by equations (1) - (4) is considered with the following data;

$$\begin{aligned}
 a(t) &= 100(e^{30t} + 1), t \in [0,1], \\
 \varphi(x) &= \sin^4(2\pi x), x \in [0,1], \\
 c(t) &= \frac{1}{2} + |t - 0.5|, t \in [0,1], \\
 e(t) &= \left(\frac{3}{16}\right)(t + 1), t \in [0,1],
 \end{aligned}$$

$$\text{and } F(x, t, u) = \frac{u}{c(t)} \left(\frac{x^2 t^{1-\alpha}}{\Gamma(2-\alpha)(t+1)} + 16\pi^2 \left(1 - 3 \frac{\cos^2(2\pi x)}{\sin^2(2\pi x)} \right) + a(t) \right), (x, t) \in [0,1] \times [0,1],$$

where $u(x, t) = (1 + t)\sin^4(2\pi x)$ is the exact solution to inverse problem. Figures 8-10 show the numerical and the exact solutions of the time-dependent source $c(t)$ and the objective function (22). The results are obtained in the same way as Example 5.1. Figure 8 explains the comparisons of numerical results of the time-dependent source $c(t)$ with exact non-smooth solution ($c(t) = \frac{1}{2} + |t - 0.5|$) with $\beta = 0$ (no regularization) and noise level $p \in \{0,1,3,5\}\%$. From the graph of this figure, we note that the numerical solution of $c(t)$ converges when $p = 0$, while the results slightly deviated from the exact ones, as the noise percentage p increases from 1% to 5% and this is expected. In Figure 9, the numerical performance of functional (22) minimization is plotted. From this figure, it can be observed a speed convergence was achieved in 7 iterations only to reach a very low value of order $O(10^{-14})$. Therefore, problem (1)-(4) is ill-posed and has to be regularized. The converge minimization of the objective function (22), as a function of the number of iterations, for $\beta \in \{10^{-2}, 10^{-3}, 10^{-4}\}$ shown in Figure 10. The associated results for $c(t)$ are presented in Figure 11 after applying Tikhonov regularization.

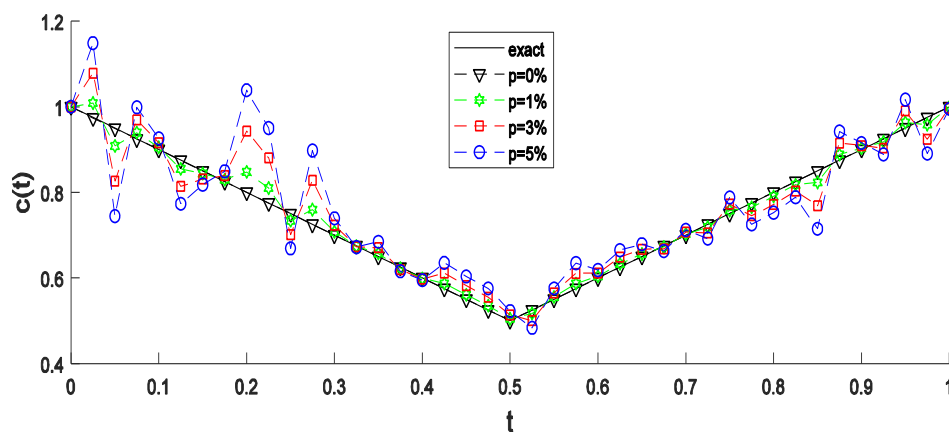


Figure 8: Reconstructed $c(t)$ for Example 5.2 with $\beta = 0$ and different amounts for p .

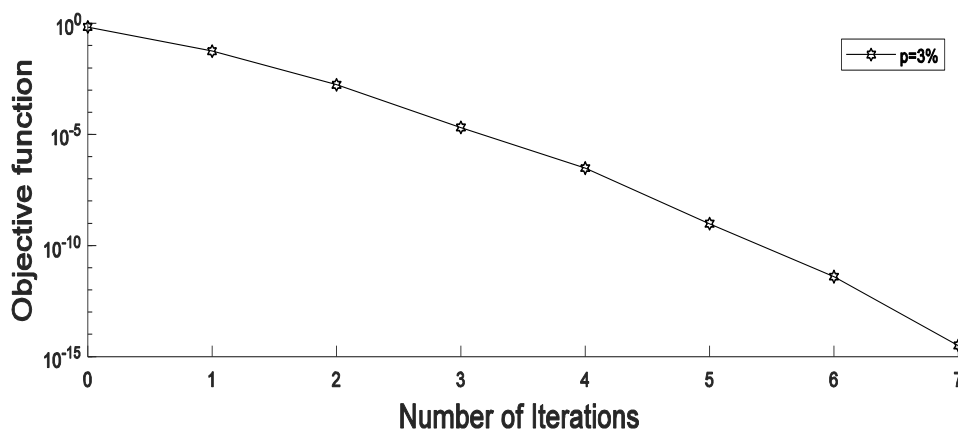


Figure 9: Objective function (22) for Example 5.2, with $\beta = 0$ and when $p = 3\%$.

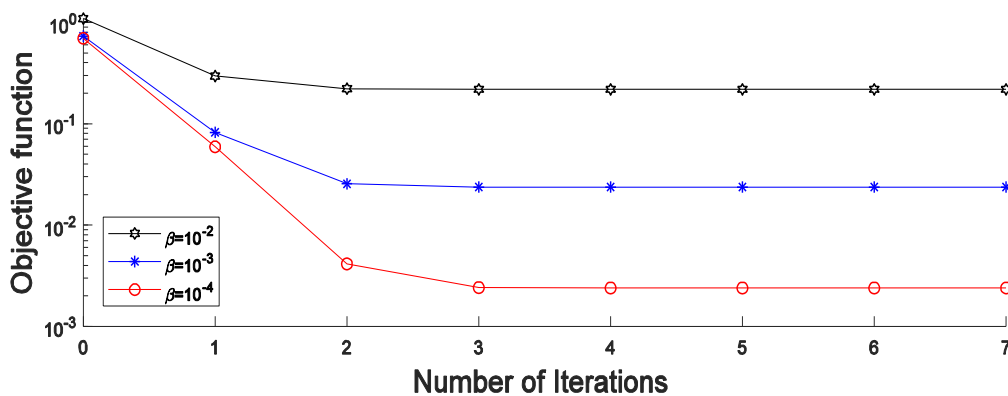


Figure 10: Objective function (22) for Example 5.2, with $p = 3\%$ and when different values for β .

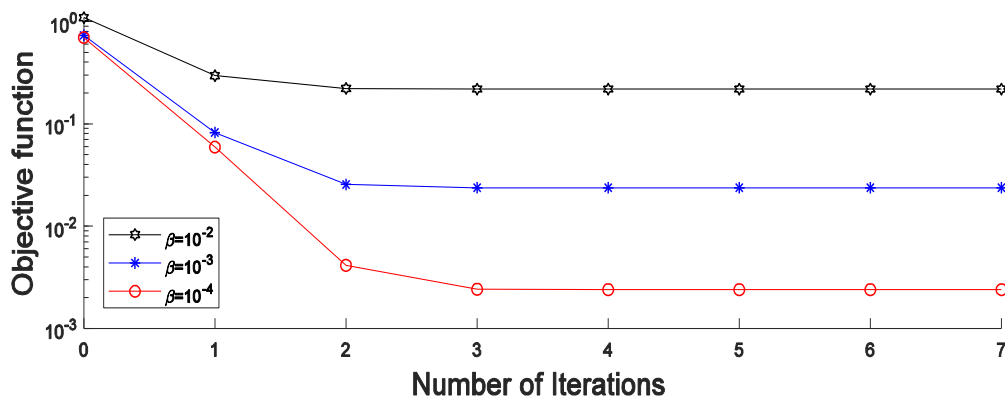
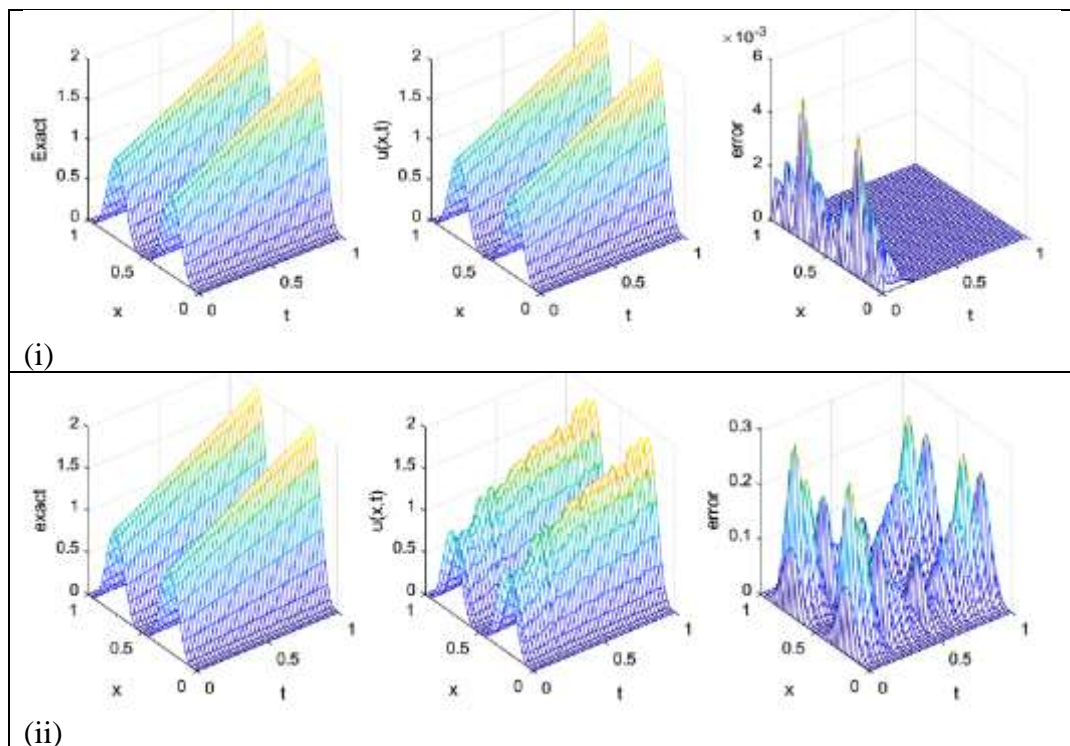


Figure 1: Reconstructed $c(t)$ with $p = 3\%$ and when different values for β for Example 5.2.

The 3D graphs of the exact and numerical solutions for $u(x, t)$, and the absolute error are plotted in Figure 12 with (i) $p = 0\%$ and $\beta = 0$, (ii) $p = 3\%$ and $\beta = 10^{-2}$, (iii) $p = 3\%$ and $\beta = 10^{-3}$, and (iv) $p = 3\%$ and $\beta = 10^{-4}$. Other details about the number of function evaluations, number of iterations, the value of the objective function (Eq.22) and the rmse of $c(t)$ in (Eq.26) are given in Table 2. From Figures 11, 12 and Table 2, it can be seen that there is a good agreement between the numerical results of $c(t)$ and $u(x, t)$ and their analytical solutions for the exact data.



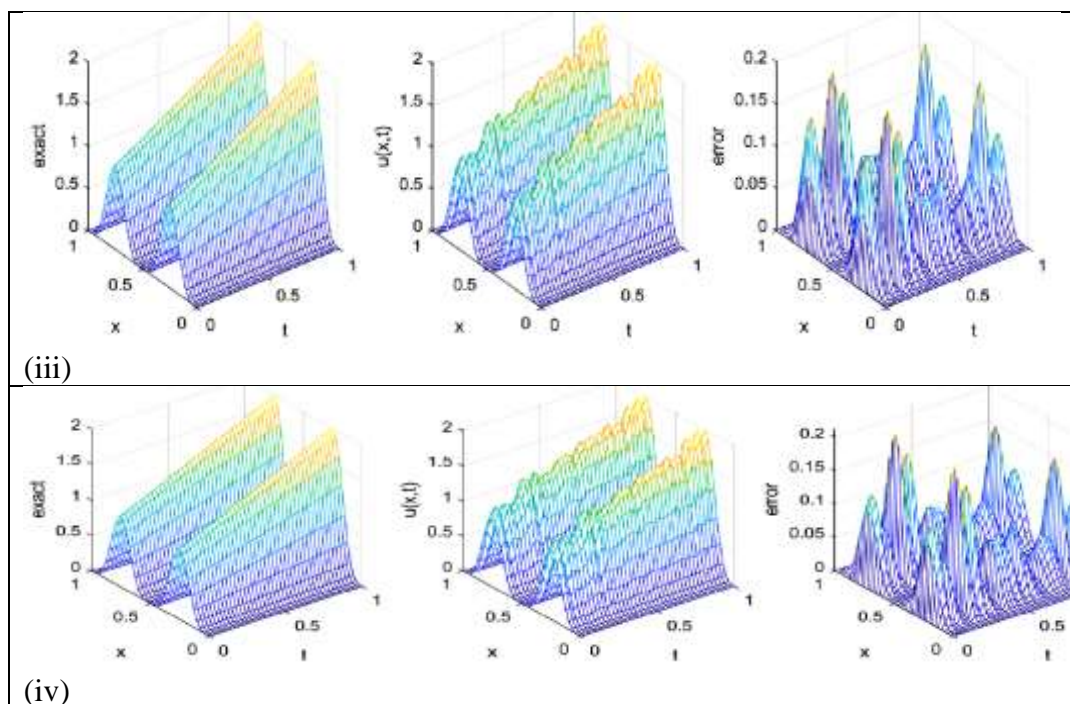


Figure 12: The exact solution, numerical solution for $u(x, t)$ and the absolute error, with (i) $p = 0\%$ and $\beta = 0$, (ii) $p = 3\%$ and $\beta = 10^{-2}$, (iii) $p = 3\%$ and $\beta = 10^{-3}$, and (iv) $p = 3\%$ and $\beta = 10^{-4}$ for Example 5.1.

Table 2: Number of iterations, number of function evaluations, value of the functional (22) and $rmse(c)$ for various amounts of noise and regularization, for Example 5.2.

	$p = 0\%$	$p = 1\%$	$p = 3\%$	$p = 5\%$
$\beta = 0$				
No. of iterations	6	6	7	7
No. of func. evaluations	294	294	336	336
Objective function value at final iteration (22)	1.02097e-13	1.02097e-13	3.13136e-15	2.1768e-16
rmse(c)	0.0002	0.0167	0.0502	0.0837
$\beta = 10^{-2}$				
No. of iterations	7	7	7	7
No. of func. evaluations	336	336	336	336
Objective function value at final iteration (22)	0.213394	0.214864	0.218397	0.222722
rmse(c)	0.0756	0.0748	0.0817	0.0975
$\beta = 10^{-3}$				
No. of iterations	6	7	7	7
No. of func. evaluations	294	336	336	336
Objective function value at final iteration (22)	0.0231095	0.0232713	0.0236612	0.0241397
rmse(c)	0.0089	0.0175	0.0490	0.0818
$\beta = 10^{-4}$				
No. of iterations	6	6	7	7
No. of func. evaluations	294	294	336	336
Objective function value at final iteration (22)	0.00233098	0.00234733	0.00238674	0.00243512
rmse(c)	0.0011	0.0166	0.0500	0.0835

6. Conclusions

In this article, a semi-linear time-fractional inverse source problem of determining temperature solution together with the time-dependent source has been investigated. The

fractional finite difference scheme (FFDS) used with the Tikhonov regularization technique for finding the stable solution of problem (1)-(4) has been utilized. Proved the stability and convergence of the proposed algorithm by the Von Neumann method (VNM). Finally, some test examples are given to validate this method.

Reference

- [1] Adam Kubica, Katarzyna Ryszewska, and Masahiro Yamamoto. *Time-Fractional Differential Equations: A Theoretical Introduction*. Springer, 2020.
- [2] Miomir S. Stanković, Anatoly Kilbas, Hari M. Srivastava, and Juan J. Trujillo: Theory and applications of fractional differential equations, Elsevier science, Amsterdam, 2006. *Facta Universitatis-series: Electronics and Energetics*, vol.24, no.1, pp.141–143, 2011.
- [3] Changpin Li and Fanhai Zeng. *Numerical methods for fractional calculus*, volume 24. CRC Press, 2015.
- [4] Qutaiba W. Ibraheem and M.S. Hussein. Determination of time-dependent coefficient in time fractional heat equation. *Partial Differential Equations in Applied Mathematics*, page 100492, 2023.
- [5] M.S. Hussein and Daniel Lesnic. Simultaneous determination of time and space-dependent coefficients in a parabolic equation. *Communications in Nonlinear Science and Numerical Simulation*, vol.33, pp.194–217, 2016.
- [6] Mohammed Qassim and M.S. Hussein. Numerical solution to recover time-dependent coefficient and free boundary from nonlocal and Stefan type overdetermination conditions in heat equation. *Iraqi Journal of Science*, vol.62, no.3, pp. 950–960, 2021.
- [7] M.S. Hussein. *Coefficient identification problems in heat transfer*. PhD thesis, University of Leeds, 2016.
- [8] M.J. Huntul and M.S. Hussein. Simultaneous identification of thermal conductivity and heat source in the heat equation. *Iraqi Journal of Science*, vol.62, no.6, pp.1968–1978, 2021.
- [9] Igor Podlubny, Aleksei Chechkin, Tomas Skovranek, YangQuan Chen, and Blas M Vinagre Jara. Matrix approach to discrete fractional calculus II: partial fractional differential equations. *Journal of Computational Physics*, vol.228, no.8, pp.3137–3153, 2009.
- [10] Farah Anwer and M.S. Hussein. Retrieval of timewise coefficients in the heat equation from nonlocal overdetermination conditions. *Iraqi Journal of Science*, vol.63, no.3, pp.1184– 1199, 2022.
- [11] Sara Salim Weli and M.S. Hussein. Numerical determination of thermal conductivity in heat equation under nonlocal boundary conditions and integral as over specified condition. *Iraqi Journal of Science*, vol.63, no.11, pp. 4944–4956, 2022.
- [12] R Faizi and R Atmania. An inverse source problem of a semilinear time-fractional reaction–diffusion equation. *Applicable Analysis*, pages 1–21, 2022.
- [13] Wei and ZQ Zhang. Reconstruction of a time-dependent source term in a time-fractional diffusion equation. *Engineering Analysis with Boundary Elements*, vol.37, no.1, pp.23– 31, 2013.
- [14] Ying Zhang and Xiang Xu. Inverse source problem for a fractional diffusion equation. *Inverse problems*, vol.27, no.3, pp.035010, 2011.
- [15] Wenyan Wang, Masahiro Yamamoto, and Bo Han. Numerical method in reproducing kernel space for an inverse source problem for the fractional diffusion equation. *Inverse Problems*, vol.29, no.9, pp.095009, 2013.
- [16] Ting Wei and Jungang Wang. A modified quasi-boundary value method for an inverse source problem of the time-fractional diffusion equation. *Applied Numerical Mathematics*, vol.78, pp.95–111, 2014.
- [17] Salih Tatar and Suleyman Ulusoy. An inverse source problem for a one-dimensional space–time fractional diffusion equation. *Applicable Analysis*, vol.94, no.11, pp.2233–2244, 2015.
- [18] Huy Tuan Nguyen, Dinh Long Le, et al. Regularized solution of an inverse source problem for a time fractional diffusion equation. *Applied Mathematical Modelling*, vol.40, no.19-20, pp.8244–8264, 2016.
- [19] Nguyen Huy Tuan and Erkan Nane. Inverse source problem for time-fractional diffusion with discrete random noise. *Statistics & Probability Letters*, vol.120, pp.126–134, 2017.

- [20] Daijun Jiang, Zhiyuan Li, Yikan Liu, and Masahiro Yamamoto. Weak unique continuation property and a related inverse source problem for time-fractional diffusion-advection equations. *Inverse Problems*, vol.33, no.5, pp.055013, 2017.
- [21] Yong-Ki Ma, P Prakash, and A Deiveegan. Generalized Tikhonov methods for an inverse source problem of the time-fractional diffusion equation. *Chaos, Solitons & Fractals*, vol.108, pp.39–48, 2018.
- [22] Xiangtuan Xiong and Xuemin Xue. A fractional Tikhonov regularization method for identifying a space-dependent source in the time-fractional diffusion equation. *Applied Mathematics and Computation*, vol.349, pp.292–303, 2019.
- [23] Smina Djennadi, Nabil Shawagfeh, MS Osman, J.F. Gomez-Aguilar, Omar Abu Arqub, et al. The Tikhonov regularization method for the inverse source problem of time fractional heat equation in the view of ABC-fractional technique. *Physica Scripta*, vol.96, no.9, pp.094006, 2021.
- [24] Smina Djennadi, Nabil Shawagfeh, and Omar Abu Arqub. A numerical algorithm in reproducing kernel-based approach for solving the inverse source problem of the time–space fractional diffusion equation. *Partial Differential Equations in Applied Mathematics*, vol.4, pp.100164, 2021.
- [25] Songshu Liu, Fuquan Sun, and Lixin Feng. Regularization of inverse source problem for fractional diffusion equation with Riemann–Liouville derivative. *Computational and Applied Mathematics*, vol.40, no.4, pp.112, 2021.
- [26] Ting Wei and Yuhua Luo. A generalized quasi-boundary value method for recovering a source in a fractional diffusion-wave equation. *Inverse Problems*, vol.38, no.4, pp.045001, 2022.
- [27] Tahereh Molaee and Alimardan Shahrezaee. Numerical solution of an inverse source problem for a time-fractional PDE via direct meshless local Petrov–Galerkin method. *Engineering Analysis with Boundary Elements*, vol.138, pp.211–218, 2022.
- [28] Ebru Ozbilge and Ali Demir. Inverse problem for a time-fractional parabolic equation. *Journal of Inequalities and Applications*, vol.2015, pp.1–9, 2015.
- [29] Keith A Woodbury. *Inverse engineering handbook*. CRC press, 2002.
- [30] A. Taghavi, A. Babaei, and A. Mohammadpour. A stable numerical scheme for a time fractional inverse parabolic equation. *Inverse Problems in Science and Engineering*, vol.25, no.10, pp.1474–1491, 2017.
- [31] William F. Ames. *Numerical methods for partial differential equations*. Academic press, 2014.
- [32] Santos B Yuste and Joaquin Quintana-Murillo. A finite difference method with non-uniform timesteps for fractional diffusion equations. *Computer Physics Communications*, vol.183, no.12, pp.2594–2600, 2012.
- [33] G. D. Smith. *Numerical solution of partial differential equations: finite difference methods*. Oxford university press, 1985.
- [34] Barhoom, N.S.S. and Al-Nassir, S., 2021. Dynamical behaviors of a fractional-order three dimensional prey-predator model. *Abstract and Applied Analysis*. vol. 2021, , Article ID 1366797, pp. 1-10.
- [35] Mathworks. Documentation optimization toolbox. www.Mathworks.com.2022.